Electrical Properties of $(Ba_{0.27}CaSr)(Zr_{0.95}Ti_{0.05})O_3$ Dielectric Ceramic with C0G Temperature Characteristics

Hong Sun Lee and Jung Rag Yoon (ID)

R&D Center, Samwha Capacitor, Seoul 08788, Korea

Abstract: In this study, the electrical properties of a C0G (class 1 ceramic) dielectric composition with internal reducibility, specifically $(Ba_{0.27}CaSr)(Zr_{0.95}Ti_{0.05})O_3$, were investigated by fixing Ba at the A site and varying the Ca/Sr molar ratio. The potential application of this composition in high-permittivity C0G MLCCs was examined. The powder was calcined at 1,150°C for 2 hours, as determined by TG-DTA analysis, and the resulting powder was ground to achieve a particle size (D_{50}) of 0.35 to 0.4 µm and a specific surface area (BET) of 4.5 to 5.0 g/m². With a Ca/Sr molar ratio of 0.3, the composition $(Ba_{0.27}Ca_{0.17}Sr_{0.56})(Zr_{0.95}Ti_{0.05})O_3$ exhibited electrical properties with a permittivity of 41.9, a loss of less than 0.008%, and an insulation resistance exceeding 2.2×10^{13} Ω. The feasibility of using this composition for high-capacitance C0G MLCCs was confirmed.

Keywords: Dielectric properties, Multi-layer ceramic capacitor, Insulation resistance, C0G

1. INTRODUCTION

The demand for multilayer ceramic capacitors (MLCCs), which are key components in the electronics industry, has significantly increased with the sector's advancements. Recently, the emergence of electronic technologies such as the Internet of Things (IoT), cloud computing, and artificial intelligence (AI), along with the expansion of the eco-friendly automobile market has led to a rapid surge in the usage of MLCCs.

The demand for C0G MLCCs, which feature high-temperature stability and low loss at high frequencies, is increasing in response to the needs for higher voltage, higher frequency, and higher efficiency in power conversion circuits of electric vehicles. In particular, with the application of wide bandgap power semiconductors based on SiC and GaN, there is a growing need for stable electrical characteristics at high temperatures and high voltages, as well as low-loss characteristics at high frequencies due to the increase in switching speeds [1-3].

To meet these characteristics, dielectric materials for MLCCs with internal electrodes such as Ag-Pd, Pd, etc., have employed materials like $MgTiO_3$-$CaTiO_3$ and BaO-Nd_2O_3-TiO_2 [2-5]. However, these dielectric materials present issues such as increased dielectric loss or decreased insulation resistance due to the generation of oxygen vacancies within the lattice during sintering in a reducing atmosphere. When using base metals such as Ni or Cu as internal electrodes, a reducing atmosphere during sintering is necessary to prevent oxidation of the internal electrodes. Thus, dielectric materials with high resistance to reduction are required. Considering high capacitance and cost-effectiveness, ceramics such as $CaZrO_3$, $(CaSr)ZrO_3$, and $(CaSr)(ZrTi)O_3$ are used as dielectrics for MLCCs that can be sintered in a reducing atmosphere [4-8].

In $(CaSr)(ZrTi)O_3$-based ceramics, it is reported that as the

✉ Jung Rag Yoon; yoonjungrag@samwha.com

Ca/Sr molar ratio increases, lattice distortion decreases, the sintering temperature is reduced, and impurity phases such as ZrO_2 or $CaZr_4O_9$ are observed, leading to increased dielectric loss [9-12]. While increasing the Ti content at the B site improves the dielectric constant and temperature characteristics, it also tends to significantly deteriorate temperature stability. To obtain raw materials suitable for high-capacitance MLCCs with high dielectric constants and C0G temperature characteristics, the composition (BaCaSr) $(ZrTi)O_3$ was selected, leveraging $BaZrO_3$ (dielectric constant: 36), which has a relatively higher dielectric constant compared to $CaZrO_3$ (dielectric constant: 27) and $SrZrO_3$ (dielectric constant: 30). The aim is to achieve both a high dielectric constant and stable temperature characteristics. According to Levin et al., the addition of $CaZrO_3$ to a $BaZrO_3$ composition results in an increase in dielectric constant from 36 to 53, along with changes in temperature characteristics and dielectric loss [13].

In this study, the electrical properties of the dielectric composition $(BaCaSr)(ZrTi)O_3$, which has an ABO_3 perovskite structure, were investigated with a fixed Ba content at the A site while varying the Ca/Sr molar ratio. The potential applicability of this material for Ni-MLCCs with high dielectric constants and C0G characteristics was also researched.

2. EXPERIMENTAL

In this study, high-purity powders of $BaCO_3$ (99.9%, Kojundo Chemical Laboratory Co., Ltd.) $SrCO_3$ (99.9%, Kojundo Chemical Laboratory Co., Ltd.), $CaCO_3$ (99.8%, Kojundo Chemical Laboratory Co., Ltd.), ZrO_2 (99.9%, Kojundo Chemical Laboratory Co., Ltd.), and TiO_2 (99.85%, Kojundo Chemical Laboratory Co., Ltd.) were used as starting materials for the $(BaCaSr)(ZrTi)O_3$ experiments. The powders were weighed according to the compositional ratios, then ball-milled for 24 hours using zirconia balls and alcohol, followed by drying. The dried powders were calcined at 1,150°C for 2 hours to synthesize $(BaCaSr)(ZrTi)O_3$ powder. To improve the electrical properties, 0.15 wt% each of MnO, Al_2O_3, and MoO_3 were added to the calcined powder, and 1 wt% of $(Ba_{0.4}Ca_{0.6})SiO_3$ glass powder was added to lower the sintering temperature. The calcined powder, additives, glass powder, zirconia balls, and deionized water were ground in a nano mill,

followed by drying. The dried powder was mixed with polyvinyl butyral (PVB, 5 wt%) as a binder and then pressed into Φ 15×1 mm pellets under 200 MPa pressure. These pellets were sintered at 1,280~1,320°C for 2 hours in a reducing atmosphere (oxygen partial pressure of 10^{-11}~10^{-13} atm) and reoxidized at 950°C for 1 hour. The sintered samples were polished to a thickness of 0.5 mm, and Ag electrodes were applied before measuring dielectric properties. The crystal structure of the ceramics was analyzed using X-ray diffraction (XRD, BRUKER, D8, ADVANCE) in the 20~80° range, and thermal analysis was performed using TG-DTA (TA Instruments DSC 250) from 25°C to 1,200°C. The dielectric properties of the samples were measured using an Impedance-Gain Phase Analyzer (HP 4194) at 1.0 MHz and 1.0 V_{rms} to determine the dielectric constant and quality factor. The temperature coefficient of capacitance (TCC) was measured from -55°C to 125°C using an LCR meter (HP 4284A) in a temperature chamber. Insulation resistance was measured using a high resistance meter (HP 4339B) after applying 100 V for 60 seconds. The MLCCs were fabricated using a standard multilayer ceramic processing technique.

3. RESULTS AND DISCUSSION

Figure 1 shows the TG/DTA curve of $(Ba_{0.27}Ca_{0.17}Sr_{0.56})$ $(Zr_{0.95}Ti_{0.05})O_3$ powder. The curve indicates that the $BaCO_3$, $CaCO_3$, and $SrCO_3$ powders used as starting materials undergo chemical decomposition reactions with ZrO_2 and TiO_2 as the temperature increases, forming $BaZrO_3$, $CaZrO_3$, $SrZrO_3$, $CaTiO_3$, secondary phases, and CO_2. A sharp exothermic peak is observed between 1,000°C and 1,040°C. The weight loss observed in the 600°C to 1,100°C range can be attributed to the volatilization of CO_2 during the formation of $BaZrO_3$, $CaZrO_3$, $SrZrO_3$, and $CaTiO_3$ phases, as well as the decomposition of any residual organic materials in the powder. Based on the results of the TG-DTA analysis, and considering the particle size distribution and crystallinity required for manufacturing multilayer ceramic capacitors, the calcination temperature was set at 1,150°C for 2 hours. The final powder, intended for use in multilayer ceramic chip capacitors, was processed using milling equipment to achieve a particle size (D_{50}) of 0.35 to 0.4 μm and a specific surface area (BET) of 4.5 to 5.0 m²/g.
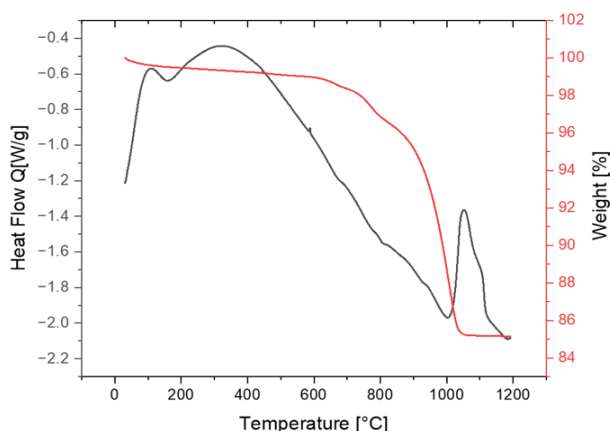
Fig. 1. TG-DTA curves for mixture of $(Ba_{0.27}Ca_{0.17}Sr_{0.56})(Zr_{0.95}Ti_{0.05})O_3$ powder.

Fig. 2. XRD diffraction patterns according to the Ca/Sr mol ratio in $(Ba_{0.27}CaSr)(Zr_{0.95}Ti_{0.05})O_3$ [(a) Ca/Sr: 0.1, (b) Ca/Sr: 0.3, (c) Ca/Sr: 0.4, and (d) Ca/Sr: 0.7].

Figure 2 shows the XRD analysis results of $(Ba_{0.3}CaSr)(Zr_{0.95}Ti_{0.05})O_3$ ceramics sintered at 1,320°C for 4 hours in a reducing atmosphere, revealing the effects of the Ca/Sr ratio. The analysis indicates that the primary phase is orthorhombic (Pnma), characteristic of a perovskite structure with both orthorhombic and cubic phases. These results were confirmed by indexing against the standard XRD patterns for $BaZrO_3$ (JCPDS: 074-1299), $SrZrO_3$ (JCPDS: 44-0161), and $CaZrO_3$ (JCPDS: 35-0645). The XRD results show that with an increase in the Ca/Sr ratio, the main peak (121) shifts to lower angles, indicating an increase in unit cell volume based on lattice constant measurements. Additionally, secondary phases become more prominent as the Ca/Sr molar ratio increases, which is consistent with previous findings that suggest the formation of secondary phases such as ZrO_2 or $CaZr_4O_9$ in stoichiometric $(CaSr)(ZrTi)O_3$ compositions [9,10]. It has been reported that secondary phases such as ZrO_2 or $CaZr_4O_9$, which appear in X-ray diffraction patterns, do not significantly affect the initial dielectric properties. However, these phases are known to cause a degradation in insulation resistance, leading to issues with the long-term reliability of MLCCs.

Figure 3 shows the SEM analysis of $(Ba_{0.27}Ca_{0.17}Sr_{0.56})(Zr_{0.95}Ti_{0.05})O_3$ ceramics sintered at 1,320°C for 2 hours. The SEM images reveal a uniform microstructure with a median grain size (D_{50}) of approximately 2 μm. For the production of high-capacitance C0G MLCCs, it is essential that the dielectric thickness is less than 4 μm after sintering. Furthermore, a reduced grain size is beneficial as it improves the dielectric breakdown voltage under high electric fields.
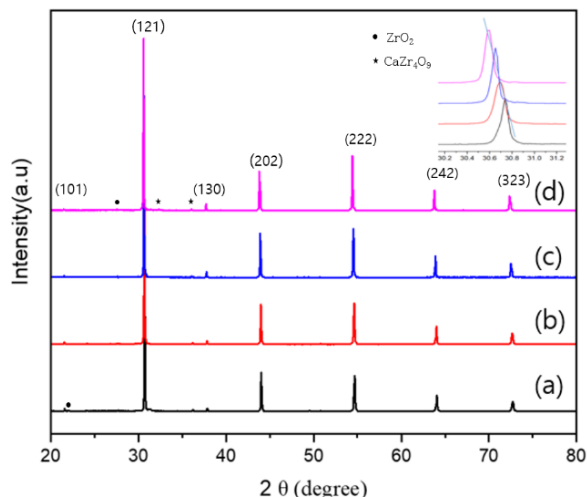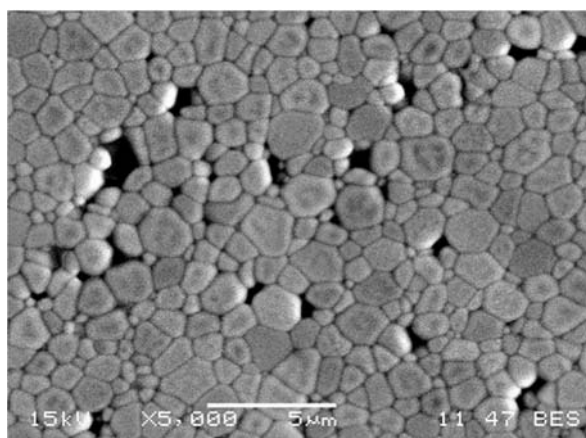

Fig. 3. SEM image of the of $(Ba_{0.27}Ca_{0.17}Sr_{0.56})(Zr_{0.95}Ti_{0.05})O_3$ ceramic by sintered at 1,320°C for 2 hr.

Figure 4 presents the results of dielectric constant and dielectric loss for $(Ba_{0.27}CaSr)(Zr_{0.95}Ti_{0.05})O_3$ ceramics sintered for 2 hours at temperatures ranging from 1,280°C to 1,320°C, as a function of the Ca/Sr molar ratio. The dielectric constant exceeds 41, which can be attributed to the formation of $BaZrO_3$ and $(BaCa)ZrO_3$ phases, both of which exhibit high dielectric constants due to the addition of Ba^{2+} at the A site. As the Ca/Sr molar ratio increases, the dielectric constant also increases. This behavior is likely due to the ionic polarization and rattling effect [9] within the ABO_3 perovskite structure, caused by the difference in ionic radii between Ca^{2+} (1.00 Å)

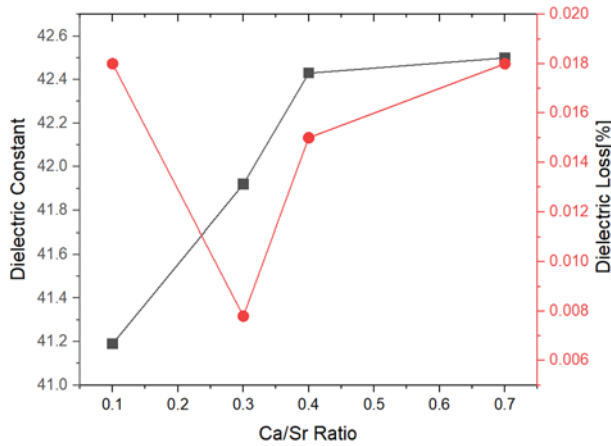**Fig. 4.** Dielectric constant and loss according to the Ca/Sr mol ratio in $(Ba_{0.27}CaSr)(Zr_{0.95}Ti_{0.05})O_3$.

Fig. 5. TCC and insulation resistance according to the Ca/Sr mol ratio in $(Ba_{0.27}CaSr)(Zr_{0.95}Ti_{0.05})O_3$.

and Sr^{2+} (1.16 Å), which leads to an increase in unit cell volume and induces polar displacement.

The dielectric loss remains below 0.018%, demonstrating excellent low-loss characteristics suitable for C0G MLCCs compositions. The optimal performance is observed at a Ca/Sr molar ratio of 0.3. These results are believed to be due to the compensatory effects of Mn and Al ions, which act as donors and acceptors to balance conduction electrons. This compensation reduces the defect concentration caused by oxygen vacancies during sintering in a reducing atmosphere, preventing the migration of oxygen vacancy defects even under an applied external field, rather than being solely attributed to the influence of the Ca/Sr molar ratio.

Figure 5 shows the temperature coefficient of capacitance (TCC) and insulation resistance of $(Ba_{0.27}CaSr)(Zr_{0.95}Ti_{0.05})O_3$ ceramics sintered for 2 hours at temperatures ranging from 1,280°C to 1,320°C, as a function of the Ca/Sr molar ratio. The TCC results demonstrate that the C0G characteristics (temperature range: -55°C to 125°C, capacitance variation within ±30 ppm/°C) are satisfied, regardless of the Ca/Sr molar ratio. However, as the Ca/Sr ratio increases, the TCC shifts from the negative toward the positive direction. This behavior is influenced by the dielectric constant (ε_r) and polarizability (α), as shown in equation (1). The dielectric constant and polarizability of the $BaZrO_3$, $(BaCa)ZrO_3$, and $CaTiO_3$ phases formed during sintering in the $(Ba_{0.27}CaSr)$ $(Zr_{0.95}Ti_{0.05})O_3$ ceramics exhibit a correlation with the temperature coefficient of the dielectric constant.

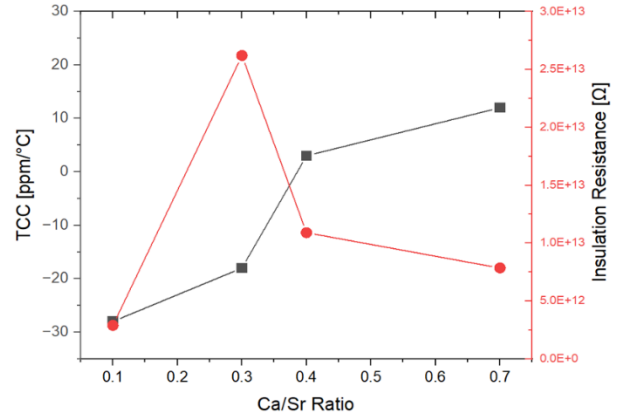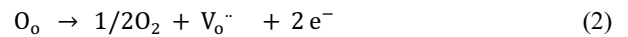$$TC_\varepsilon = \frac{\varepsilon_r}{3}\left(\frac{1}{\alpha}\frac{\partial \alpha}{\partial T} - 3\alpha_L\right) \tag{1}$$

Where, α is the thermal expansion coefficient of the ceramic.

The insulation resistance behavior in a reducing atmosphere with low oxygen partial pressure can be described by equation (2), where oxygen vacancies ($V_o^{\cdot\cdot}$) and electrons (e^-) are generated.

$$O_o \rightarrow 1/2O_2 + V_o^{\cdot\cdot} + 2\,e^- \tag{2}$$

Here, O_0 represents the oxygen in the $(BaCaSr)(ZrTi)O_3$ composition.

The variation in insulation resistance as a function of the Ca/Sr molar ratio in $(Ba_{0.27}CaSr)(Zr_{0.95}Ti_{0.05})O_3$ shows that the optimal properties are observed at a Ca/Sr ratio of 0.3, similar to the dielectric loss characteristics. In this experiment, the addition of the transition metal Mn, acting as an acceptor, is believed to contribute to the reduction of mobile oxygen vacancy defects by forming defect associations between oxygen vacancies and Mn^{2+}, thereby improving insulation properties in the high-dielectric constant composition. Additionally, the presence of Al^{3+} ions, functioning as donors, reduces conduction electrons, resulting in excellent insulation resistance across the entire range of Ca/Sr molar ratios [14]. During sintering, Mo^{6+} ions are reduced to Mo^{4+} or Mo^{3+} ions, which are substituted into A-site or B-site ion positions,
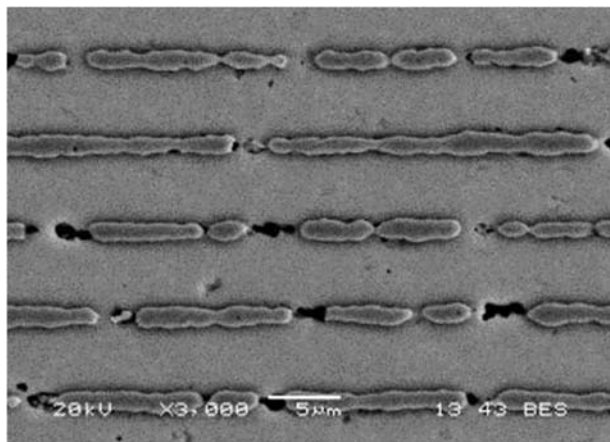
Fig. 6. SEM image of the MLCC with $(Ba_{0.27}CaSr)(Zr_{0.95}Ti_{0.05})O_3$ composition by sintered at 1,280°C for 2 hr.

thereby compensating for valence and enhancing insulation resistance properties. This outcome is similar to the mechanism observed in reduced-atmosphere MLCCs using $BaTiO_3$, where rare-earth additives such as Y_2O_3 and Dy_2O_3 substitute into A-site or B-site positions, leading to improved insulation resistance and reliability [15,16].

Figure 6 shows the microstructure of a multilayer ceramic capacitor (MLCC) fabricated using the $(Ba_{0.27}CaSr)(Zr_{0.95}Ti_{0.05})O_3$ composition with a Ni internal electrode. The image demonstrates excellent sintering characteristics and a well-developed microstructure, even under a reducing atmosphere.

4. CONCLUSION

In this study, we developed a dielectric composition suitable for high-capacitance multilayer ceramic capacitors (MLCCs) with C0G temperature characteristics, specifically designed for the LLC resonant circuit of electric vehicles. Under reducing conditions, we achieved a composition $(Ba_{0.27}CaSr)(Zr_{0.95}Ti_{0.05})O_3$ with a dielectric constant of 41.9, loss of less than 0.008%, and insulation resistance greater than 2.2×10^{13} ohms. Powder synthesis was conducted at 1,150°C for 2 hours, followed by grinding to achieve a particle size distribution (D_{50}) of 0.35~0.4 μm and a specific surface area (BET) of 4.5~5.0 g/m^2. We confirmed the feasibility of producing high-capacitance C0G MLCCs using this powder for potential applications.

ORCID

Jung Rag Yoon   https://orcid.org/0000-0002-9206-8701

REFERENCES

[1] K. Hong, T. H. Lee, J. M. Suh, S. H. Yoon, and H. W. Jang, *J. Mater. Chem. C*, **7**, 9782 (2019).
doi: https://doi.org/10.1039/c9tc02921d

[2] I. Seo, H. W. Kang, and S. H. Han, *J. Korean Inst. Electr. Electron. Mater. Eng.*, **35**, 103 (2022).
doi: https://doi.org/10.4313/JKEM.2022.35.2.1

[3] A. Zeb and S. J. Milne, *J. Mater. Sci.: Mater. Electron.*, **26**, 9243 (2015).
doi: https://doi.org/10.1007/s10854-015-3707-7

[4] T. Yamagushi, Y. Komatsu, T. Otobe, and Y. Murakami, *Ferroelectrics*, **27**, 273 (1980).
doi: https://doi.org/10.1080/00150198008226116

[5] S. H. Lee, M. K. Kim, H. K. Kim, and J. R. Yoon, *J. Ceram. Process. Res.*, **18**, 722 (2017).
doi: https://doi.org/10.36410/jcpr.2017.18.10.722

[6] M. Chen, J. L. Liao, and H. I. Hsiang, *Ceram. Int.*, **48**, 28023 (2022).
doi: https://doi.org/10.1016/j.ceramint.2022.06.107

[7] Q. Pang, Y. Li, F. Yang, Z. Liu, X. Li, H. Cheng, S. Sun, Y. Chen, and G. Wang, *Ceram. Int.*, **49**, 8598 (2023).
doi: https://doi.org/10.1016/j.ceramint.2022.11.037

[8] F. Shi, K. Liang, and Z. M. Qi, *J. Mater. Res.*, **31**, 3249 (2016).
doi: https://doi.org/10.1557/jmr.2016.340

[9] L. Duan, J. Zhang, J. Li, H. Xiang, Y. Tang, X. Luo, and L. Fang, *J. Eur. Ceram. Soc.*, **43**, 4066 (2023).
doi: https://doi.org/10.1016/j.jeurceramsoc.2023.03.028

[10] A. Devoe, H. Trinh, and F. Dogan, *Int. J. Appl. Ceram. Technol.*, **20**, 3140 (2023).
doi: https://doi.org/10.1111/ijac.14432

[11] J. Joseph, T. M. Vimala, K.C.J. Raju, and V.R.K. Murthy, *Jpn. J. Appl. Phys.*, **35**, 179 (1996).
doi: https://doi.org/10.1143/jjap.35.179

[12] N.T.K. Ngan and S. Cho, *J. Korean Inst. Electr. Electron. Mater. Eng.*, **37**, 274 (2024).

doi: https://doi.org/10.4313/JKEM.2024.37.3.5

[13] I. Levin, T. G. Amos, S. M. Bell, L. Farber, T. A. Vanderah, R. S. Roth, and B. H. Toby, *J. Solid State Chem.*, **175**, 170 (2003). doi: https://doi.org/10.1016/s0022-4596(03)00220-2

[14] X. Cheng, Y. C. Zhen, P. Zhao, K. Hui, M. Xiao, L. Guo, Z. Fu, X. Cao, L. Li, and X. Wang, *J. Am. Ceram. Soc.*, **106**, 5294 (2023). doi: https://doi.org/10.1111/jace.19168

[15] S. H. Lee, D. Y. Kim, M. K. Kim, H. K. Kim, J. H. Lee, E. Baek, and J. R. Yoon, *J. Ceram. Process. Res.*, **16**, 495 (2015). doi: https://doi.org/10.36410/jcpr.2015.16.5.495

[16] G. K. Choi, J. R. Kim, S. H. Yoon, and K. S. Hong, *J. Eur. Ceram. Soc.*, **27**, 3063 (2007). doi: https://doi.org/10.1016/j.jeurceramsoc.2006.11.037